Ocean Engineering 173 (2019) 227–234

Contents lists available at ScienceDirect

Ocean Engineering

journal homepage: www.elsevier.com/locate/oceaneng

Antifouling paint schemes for green SHIPS

A. Mukherjee[a,*], M. Joshi[b], S.C. Misra[b], U.S. Ramesh[b]

[a] Gayatri Vidya Parishad College of Engineering, Madhurawada, Visakhapatnam, 530048, India
[b] Indian Maritime University (Visakhapatnam Campus), Gandhigram, Visakhapatnam, 530015, India

ARTICLE INFO

Keywords:
Antifouling
Self polishing coatings
CFD
Invasive species
Painting schemes

ABSTRACT

Recent advances in antifouling (AF) paints in general prevent fouling in about 95% of the vessel's immersed surface. However the remaining area which amounts to 5% or less of the total area does get fouled. Although this level of fouling has marginal impact on the routine performance of the vessel it is a predominant vector for the transmigration of invasive species which is now a serious environmental concern. Virtually all ocean going vessels are coated with antifouling paints predominant among them are “Self polishing coatings”. CFD analysis conducted on various types of vessels have indicated that there are certain “hotspots” where the polishing rates are exceedingly high and would polish the AF paints at a much faster rate and ultimately result in the failure of the AF coating. A possible solution to this issue is to first identify these hotspots and suitable paint schemes/formulations are to be applied in such areas. An experimental procedure utilizing a “drum-test” apparatus can be used to compute the coating thicknesses based on wall shear stresses. Such painting schemes would prevent the premature failure of the AF coating in general and significantly reduce the risk of transmigration of invasive species in particular.

1. Introduction

The commercial shipping industry primarily uses Self-polishing copolymer (SPC) paints as anti-fouling coatings. These paints were introduced in the mid-1970s and in this class of paints the biocide is chemically bonded to a copolymer (Anderson, 1993 Hunter and Cain, 1996 Ma et al., 2017). The leaching rate of the biocide is highly controlled due to the fact that biocide is released when sea water reacts with the surface layer of the paint (Almeida et al., 2007). The SPC paints allow the application of thicker coatings with the biocide chemically bonded throughout the coating. This results in the slow and uniform release of biocides to the surface (Hellio and Yebra, 2009). The biocide release for these coatings is only a few nanometres deep and the spent layer is slowly eroded away and a new active layer develops. The popularity of these Antifouling (AF) coatings was primarily due to a controlled chemical dissolution of the paint film capable of long dry-dock intervals typically between five to seven years predictable polishing enabling tailor-made specifications by vessel/operation thin leached layers making it easy to clean and recoat good weather ability quick drying and extremely good value for money (Yebra et al., 2005 Jones, 2009).

2. Hydrodynamic forces at paint-seawater interface

The extent of polishing action in SPC paints depend primarily on the hydrodynamic forces at the paint-seawater interface. The higher the hydrodynamic forces the higher are the polishing rates. Conversely lower hydrodynamic forces at the paint-seawater interface imply lower polishing rates. This implies that at locations where the hydrodynamic forces are high the polishing rates would be high and this could result in premature depletion of the antifouling coating. Also when the hydrodynamic forces are very low such as a ship standing in port waters low polishing action would result and this would lead to insufficient biocide release at the paint-water interface (Kiil et al., 2001). In both the preceding scenarios the paint film does not offer antifouling protection. In the first case only when the paint is depleted (which takes some time) fouling takes place whereas in the second case fouling takes place almost immediately.

The practice of application of antifouling coating is that a uniform coating of a specified pre-calculated thickness is applied on the underwater hull of the vessel taking in to account the average speed of the vessel its trading routes length of stay in port etc. However shipbuilders/owners etc do not account for the fact that there are non-uniform polishing rates along the vessels hull in certain niche areas in the proximity of bow thrusters sea chest stern tube rudder shoulder water line etc that are prone to premature fouling (Camps et al., 2014). These areas are less than five percent of the total underwater area of the vessel and therefore have negligible effect as far as the operational parameters of the vessel are concerned (Drake and Lodge, 2007 Demirel et al., 2014). Although depletion of paints initiates corrosion a far more serious concern is that they are the primary vector for the transmigration of invasive species (Chan et al., 2015 Olivera and Granhag,

* Corresponding author.
E-mail address: admukh@gvpce.ac.in (A. Mukherjee).

https://doi.org/10.1016/j.oceaneng.2018.12.057
Received 9 January 2017; Received in revised form 30 October 2018; Accepted 22 December 2018

2016). Now days some paint manufactures have started suggesting variable paint thickness across the hull surface the reasons for which are unknown.

Invasive species also called as alien species or non-native species are introduced in the marine environment by human activities threatens biological diversity and ecological integrity worldwide. They can cause irreversible reduction in biodiversity by preying on or by competing or causing or carrying diseases or altering habitats of native species and threaten biodiversity by predation or competition. They can also cause serious economic and ecological damage. Some can damage shorelines man-made marine structures equipment and vessels. The UNEP has declared that the invasive species are the most serious environmental issue only next to habitat loss. Many studies show that hull fouling is the primary vector for invasive species. (Rainer, 1995; Coutts, 1999; Hewitt, 2002; Gollasch, 2002; Ashton et al., 2007 Coutts et al., 2010). Even the best maintained vessels are fouled to the extent of at least three percent of the hull area and are more than sufficient to cause the transmigration of alien species (Gollasch, 2002 Brine et al., 2013).

3. Analysis of hydrodynamic forces at fluid_hull interface

A CFD analysis of hydrodynamic flow around the hull of a tanker and a 100 passenger vessel was carried out using FLUENT software. Simulation of flow around the hull has been performed by Computational Fluid Dynamics (CFD) techniques using FLUENT. The velocity profiles and wall shear stress distribution acting on the surface of the hull have been obtained based on CFD solutions. The flow around the hull surface is governed by the incompressible form of the Navier–Stokes equation. A flow solution based on solution of the Navier-Stokes equation using standard software available in the market has been attempted (Larsson and Raven, 2010). The Reynolds-averaged form of the above momentum equation including the turbulent shear stresses is given by

$$\frac{\partial}{\partial t}(\rho\vec{V}) + \nabla.(\rho\vec{V}\vec{V}) = \nabla p + \nabla.\tau + \rho\vec{g} + \vec{F}$$

where

ρ is the fluid density
$\vec{V}$ is the fluid velocity relative to the vessel
ρ is the pressure
τ is the shear stress
$\vec{g}$ is the acceleration due to gravity
$\vec{F}$ is any other external force term

The ship was modeled from a lines plan of two existing ships. Lines plan was first drafted in AUTOCAD and it was exported TRIBON to model the 3-dimensional hull form. The 3-d models of the ships are then taken as half the original volume and a flow volume was created and meshed in ANSYS software. The flow volume is of a box shape and hull surface is inside the box to level of the draft and upper surfaces (above waterline) are trimmed (Fig. 1).

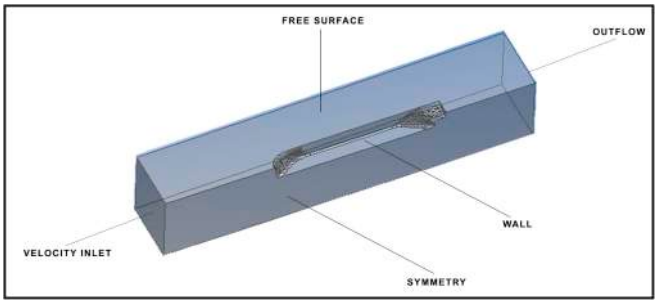

Fig. 1. Schematic description of boundary conditions.

The details of the vessels for which the flow analysis was conducted are given below.

Vessel 1

Type:	Tanker
Overall length:	220 m
Maximum draft:	12 m
Maximum speed:	16 knots

Vessel 2

Type:	100 passenger vessel
Overall length:	90 m
Maximum draft	3 m
Maximum speed:	20 knots

The boundary conditions used are schematically described below.

The fluid is assumed to enter the flow volume at an upstream boundary or inlet such that the ship appears stationary and the water flows past it. The inlet boundary velocity is set to be a fixed value equal to the velocity of the ship but in the opposite direction. The vessel's hull is set to be a wall with a no-slip condition. In order to reduce the size of the computational domain a symmetry plane is taken along the ship's centerline. In cases for which the free surface effects are small or simply not of interest the water-plane can also be assumed to be a wall with zero shear slip. The top wall is therefore taken as a free surface with a prescribed zero shear stress. The symmetry boundary condition for the scalar pressure and velocity components tangential to these boundaries is that their gradients normal to these boundaries are zero.

Standard k - $\in$ model was used to model turbulence and the details of which are given next:

The turbulence kinetic energy and its rate of dissipation is obtained from the following transport equations:

$$\frac{\partial}{\partial t}(\rho\kappa) + \frac{\partial}{\partial x_i}(\rho\kappa u_i) = \frac{\partial}{\partial x_j}[(\mu + \frac{\mu_t}{\sigma_k})\frac{\partial\kappa}{\partial x_j}] + G_k + G_b - \rho\varepsilon - Y_m + S_\kappa$$

and

$$\frac{\partial}{\partial t}(\rho\varepsilon) + \frac{\partial}{\partial x_i}(\rho\varepsilon u_i) = \frac{\partial}{\partial x_j}[(\mu + \frac{\mu_t}{\sigma_\varepsilon})\frac{\partial\varepsilon}{\partial x_j}] + C_{1\varepsilon}\frac{\varepsilon}{\kappa}(G_\kappa + C_{3\varepsilon}G_b) - C_{2\varepsilon}\rho\frac{\varepsilon^2}{\kappa} + S_\varepsilon$$

The turbulent (or eddy) viscosity is computed by the equation:

$$\mu_t = \rho C_\mu \frac{\kappa^2}{\varepsilon}$$

where $\mathbf{C}_\mu$ is a constant.

Model Constants that were used are:

$C_{1\varepsilon} = 1.44$, $C_{2\varepsilon} = 1.92$, $C_\mu = 0.09$, $\sigma_\kappa = 1.0$, $\sigma_\varepsilon = 1.3$

k is the turbulent kinetic energy
ε is the dissipation rate of kinetic energy
G_k is the generation of turbulent kinetic energy due to mean velocity gradients
G_b is the generation of kinetic energy due to buoyancy
Y_m represents the contribution of the fluctuating dilation in the compressible turbulence to overall dissipation rate
S_ε S_k are the user defined source terms for turbulent kinetic energy and its dissipation rate respectively.

Figs. 2-5 shows the computed wall shear stresses of a 200 m long tanker and Figs. 6 and 7 show the same stresses of a 100 passenger vessel. In all cases the flow of water is from bow to stern (i.e. from left to right). In each of the figures depicted there is a marked variation in

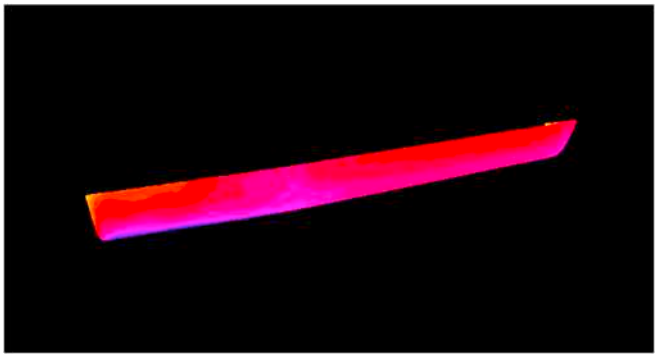

Fig. 2. Wall shear stresses of a tanker at a draft of 12 m and speed of 6 m/s (blue indicates regions of high shear stress and yellow the lowest shear stress).

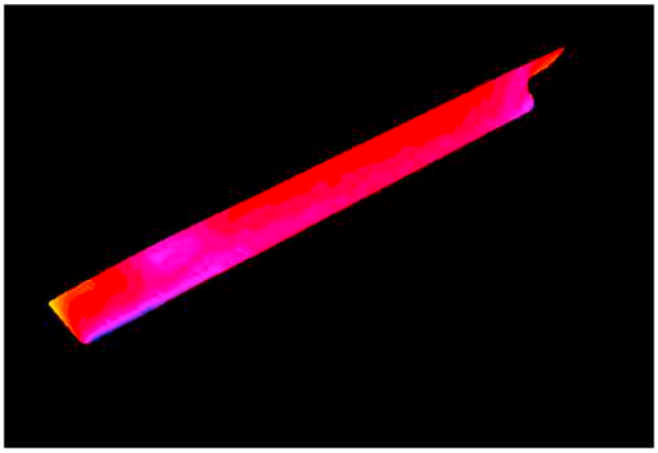

Fig. 3. Wall shear stresses of a tanker at a draft of 6 m and speed of 6 m/s (blue indicates regions of high shear stress and yellow the lowest shear stress).

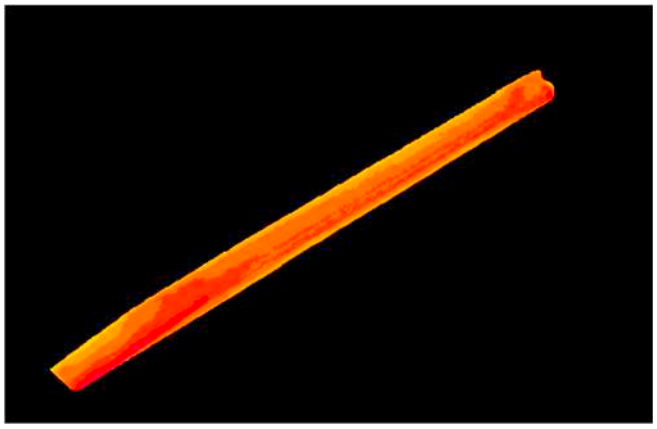

Fig. 4. Wall shear stresses of a tanker at a draft of 12 m and speed of 4 m/s (red indicates regions of high shear stress and yellow that of low shear stress).

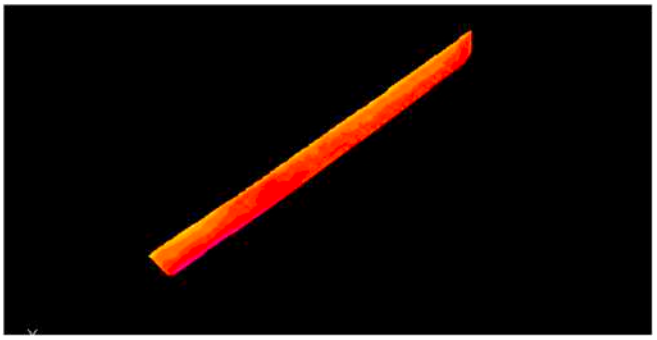

Fig. 5. Wall shear stresses of a tanker at a draft of 12 m and speed of 5 m/s (red indicates regions of high shear stress and yellow that of low shear stress).

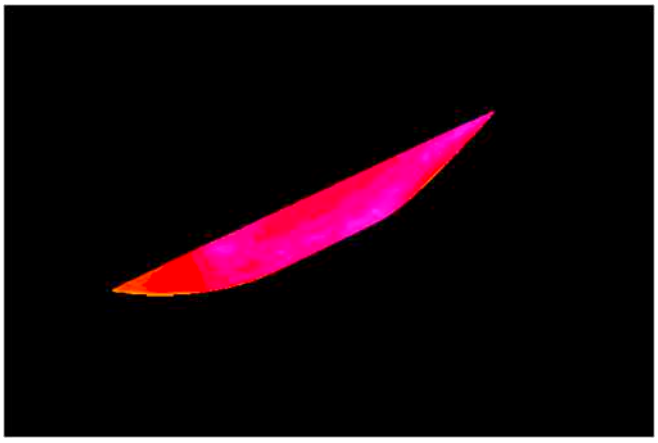

Fig. 6. Wall shear stresses of a 100 passenger vessel at a draft of 3 m and speed of 3 m/s (blue indicates regions of highest shear stress and orange that of lowest shear stress).

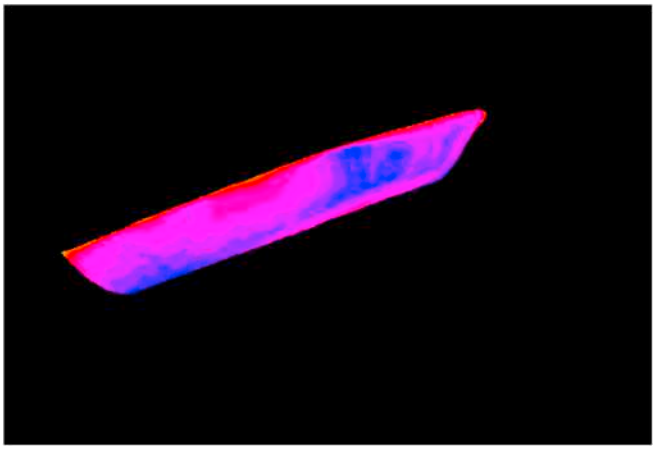

Fig. 7. Wall shear stresses of a 100 passenger vessel at a draft of 3 m and speed of 6 m/s (blue indicates regions of highest shear stress and orange that of lowest shear stress).

the wall shear stresses throughout the hull which depends on the speed the draft and the vessel shape. It can be observed that higher shear stresses (which could imply) higher paint polishing rates are only underwater and the boot top region is not a critical area for AF paint depletion. It can also be observed that stresses are high at areas of sharp curvature of the hull surface such as bilges and shoulders where wall shear stress is also high. Speed is also a primary parameter in determining wall shear stress. This is evident from Figs. 2 and 3. Areas of the vessel that experience comparatively high hydrodynamic stresses and therefore higher polishing rates show indications of premature fouling.

The current painting practice is that an antifouling coating of uniform thickness is applied without taking into considerations of the various hydrodynamic stresses. For both the tanker and the 100 passenger (PAX) vessel the computed shear stresses at the waterline and the stern have lower than average hydrodynamic stresses which indicates low polishing rates the extent of which depends on the draft speed and type of vessel. In these areas insufficient biocide delivery

results which is likely to result in premature fouling. On the other hand for the tanker in particular the shoulder of the vessel (behind the bow) experiences high wall stresses which result in higher polishing rates in comparison to the rest of the vessel. This would lead to the premature depletion of the antifouling paint and would again result in fouling much ahead of the bulk of the surface of the vessel.

Thus at low shear stress regions there could be insufficient delivery of biocides leading to premature or large fouling. Also in regions of high shear stress paint depletion is rapid leading to early initiation of fouling. It is seen that both regions of high and low shear stress lead to fouling. In case a full form ship like a tanker the regions of high shear stress can be identified as regions of large curvature which are very pronounced along the bilges and forward and aft shoulders and this happens at comparatively low speed or at low Froude number. But in case of a fine form ship like a passenger vessel the regions of sharp curvature are less with comparatively low shear stress at similar speeds (i.e. same Froude number) but shear stresses increase sharply with increase in speed or Froude number and this increase is spread over large area of the hull surface.

4. Identification of niche areas for fouling

The issue of invasive species can therefore be best addressed if fouling is further reduced or completely eliminated particularly in the niche areas of the vessel. This could be best accomplished if these areas are accurately identified and appropriate paint schemes are applied at these regions. To locate these niche areas hydrodynamic forces at the paint-water interface are to be analyzed. Fig. 8 depicts photographs of tanker on arrival at dry-dock in the regular survey schedule and therefore after 5 years of last painting. From these photographs it is evident that there is a marked depletion of AF coating in certain areas of the tanker. The fouled areas are illustrated in Fig. 9 for the entire length of the vessel. The Computational fluid dynamics (CFD) analysis shown in Fig. 10 corresponds approximately to the average operational speed and draft of tanker 1 which has a draft of 12 m and a speed of approximately 6 m per second. In this figure wall shear stresses are high along the bottom of the vertical sides of the vessel with a small region (forward and aft shoulders) extending to the boottopping zone at the forward one third of the hull length. Although there could be many factors that may contribute to the excessive paint depletion which could include structural deformation, butt welding, etc, however when compared with the dry-dock data as pictorially depicted in Fig. 8 it is observed that there does exist a fairly good correlation between regions of high wall shear stress and fouling. This is a likely indicatation that high wall shear stress results in the premature wearing of the AF protection which ultimately leads to fouling.

Passenger vessel data for actual ship has not been obtained. Since the tanker calculations and photographs show matching trends, the calculations for passenger vessel are also likely to indicate regions of high shear stress correctly.

Therefore in order to significantly minimize fouling antifouling (AF) painting schemes must take into account the uneven hydrodynamic forces at the water-hull interface. In other words if a CFD analysis is first conducted to identify areas of high wall shear stress and correlation between wall shear stress at all locations on the vessels hull with rate of antifouling paint depletion is known then the appropriate AF scheme could be applied.

5. Experiments for determiming polishing rate (the drum test apparatus)

To obtain such a correlation between wall shear stress and the rate of antifouling paint depletion the “Drum-Test” apparatus was devised designed manufactured and utilized. Ideally flow past a body to study the paint deterioration should have been simulated in an experimental set up by moving a flat plate or moving water around a stationary flat plate. However such an experiment would require a towing tank or a water tunnel (Politis et al., 2011; Politis et al., 2013). Here the flow would be linear as in case of a ship. More importantly, any paint flow test is normally carried out over a long period of time and the experimental facility has to be occupied for this test only. However, the Drum-Test apparatus utilized here is an easy to use, low cost facility where the flow is turbulent and largely tangential to the drum and at any point it is linear without any circulation or vortex generation though there could be some curvature effects.

The sketch of the drum test apparatus is shown in Fig. 11. It essentially consists of two concentric cylinders. The inner cylinder which is 250 mm in diameter rotates about a vertical shaft that is connected to a variable speed motor. The outer cylinder is 600 mm in diameter and is stationary. The gap within the inner and outer cylinders is filled with sea water. Plates coated with various antifouling paints are affixed on the inner cylinder and the inner cylinder is rotated at a known fixed speed for a predetermined time. A total of six such plates can be attached to the central drum. Each of the steel plates were cleaned with thinner (chlorinated rubber) and dried. Then the surface of the plates was mechanically cleaned to visual standards of ST3 for surface preparation. After surface preparation plate was first brush coated with a primer of 50 μm. Two coats of anticorrosive paints of 150 μm each were applied. Then tie coat of 60 μm was applied and after 4 h of drying two antifouling coats of 100 μm each were finally applied. The painting scheme was according to manufacturer's instruction. Artificial seawater was prepared by adding 3.5 g of crude salt per liter of tap water. The drum was then rotated at the pre-determined RPM for eight hours a day. The paint film thickness was measured after regular intervals using an ultrasonic paint film thickness gauge. The experiments were conducted in duplicate (i.e. two plates of the same specifications and paint thickness were attached to the drum) and the residual film thickness reported is the average of the measurements from the two plates. The drum speeds Reynolds number and wall shear stresses at which the experiments were conducted are listed below in Table 1.

Although the maximum wall shear stresses on the vessel depicted in Fig. 10 are in the range of 40–50 Pa the drum was intentionally run at speeds that correspond to shear stress that ranges between 679.8 and 1542.8 Pa in order to obtain film thicknesses that are measurable within a reasonable time.

6. Results and discussions

The results of paint film depletion versus time for various speeds of the drum are depicted in Fig. 12a to c. In Fig. 12a only two points were taken due to limitation of time whereas for Fig. 12b and c three points were available. In all cases the paint film depletion varies approximately linearly with time for a particular speed of rotation (or shear stress) which is a typical characteristic of a self polishing antifouling paint.

The wall shear stress for a particular speed on the drum has been estimated by CFD techniques by using commercially available software (FLUENT). Ideally the provision of a torque meter attached to the shaft of the drum would provide a direct measurement (and therefore a more accurate measurement) of torque. As such a meter could not be incorporated in this particular apparatus, hence, the wall shear stresses were estimated by CFD techniques. The computed wall shear stress with the rate of AF paint film depletion per day is plotted in Fig. 13 for three different AF paints.

7. Optimum painting schemes

. The residual film thicknesses are to be predicted for a length of time that corresponds to a typical dry-dock cycle of a commercial vessel which is approximately five years. This period may vary for naval vessels and vessels operating in near shore areas such as coastguard vessels. This correlation depends on a number of parameters that

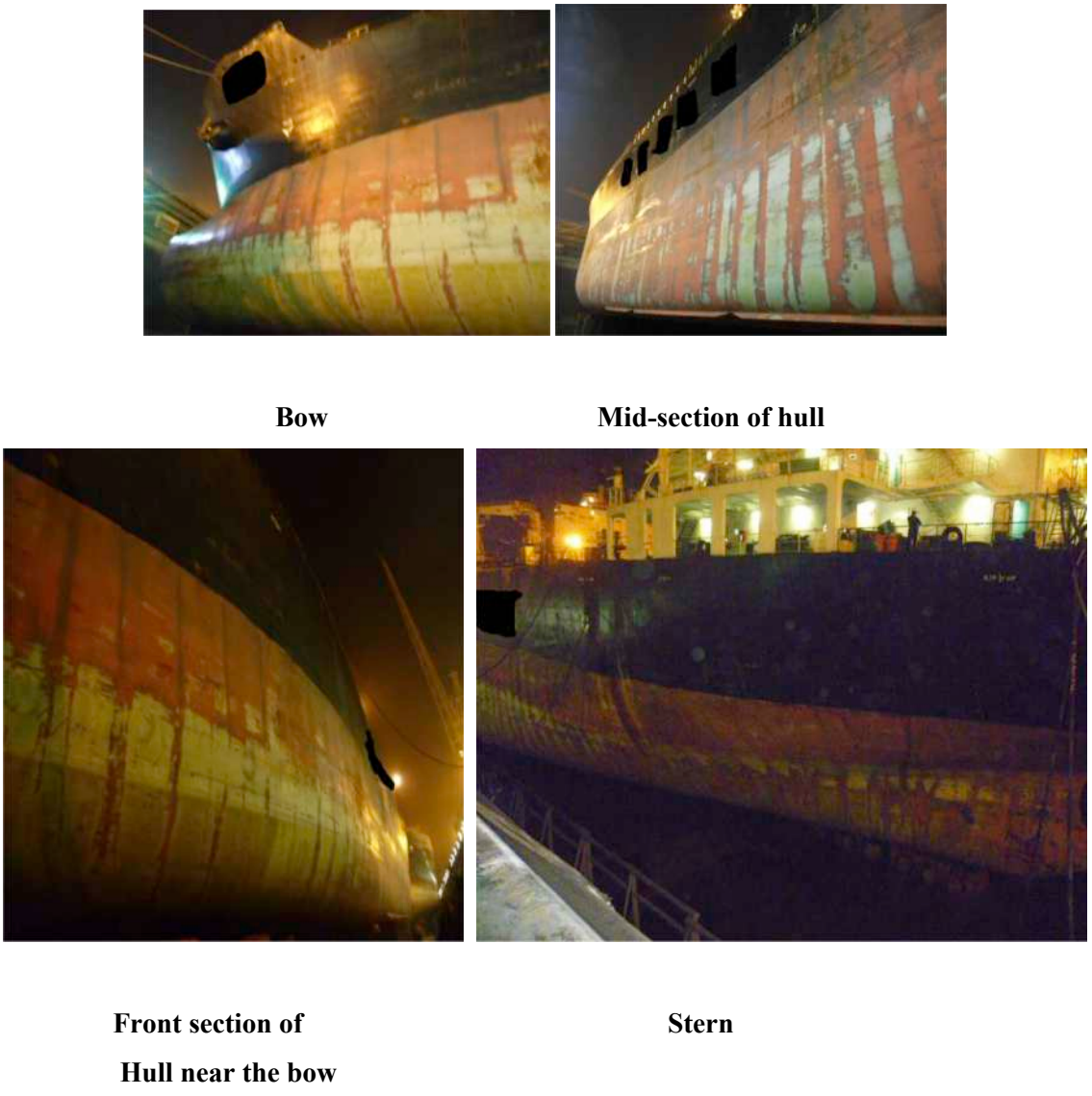

Fig. 8. Antifouling Paint Failure of tanker 1.

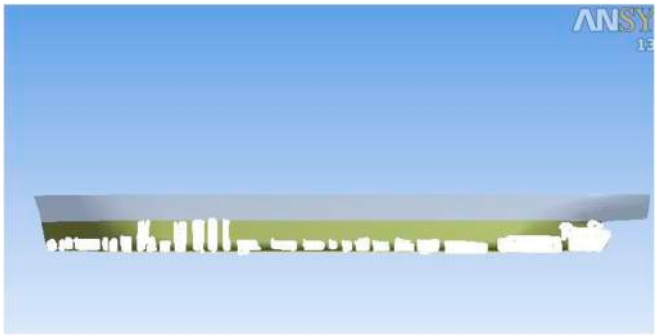

Fig. 9. Sketch of hull of predominant AF failure for tanker 1. – taken from photographs (note green indicates the underwater portion of the hull).

includes type of coating its formulation method of application backbone polymer additives etc. Thus by establishing the correlation between wall shear stresses and antifouling paint film depletion for a particular

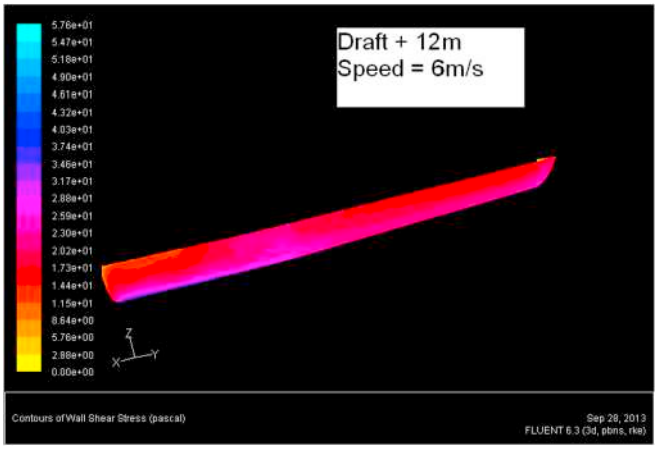

Fig. 10. Wall shear stresses of the under water portion of a tanker at a draft of 12 m and speed of 6 m/s (blue indicates regions of high shear stress and yellow the lowest shear stress) – From simulations.

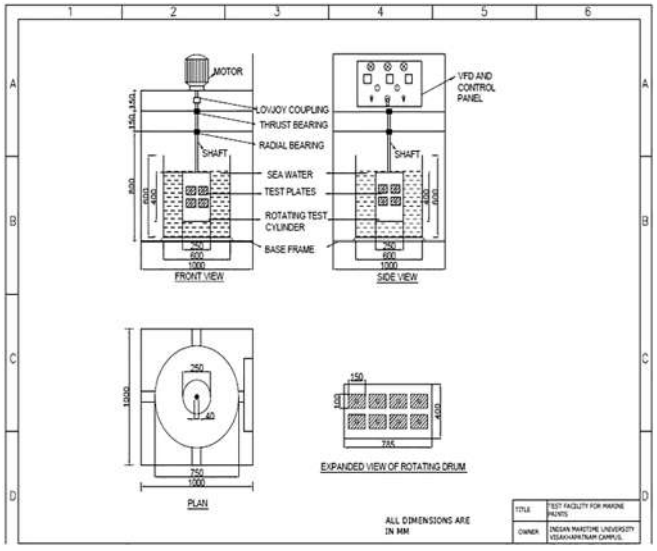

Fig. 11. Sketch of drum test apparatus.

Table 1
Hydrodynamic parameters of drum test.

No.	RPM	Linear velocity (m/s)	Reynolds number	Wall Shear Stress (Pa)
1.	450	5.89	0.864×10^6	679.8
2.	550	7.19	1.056×10^6	1181.8
3.	690	9.07	1.331×10^6	1542.8

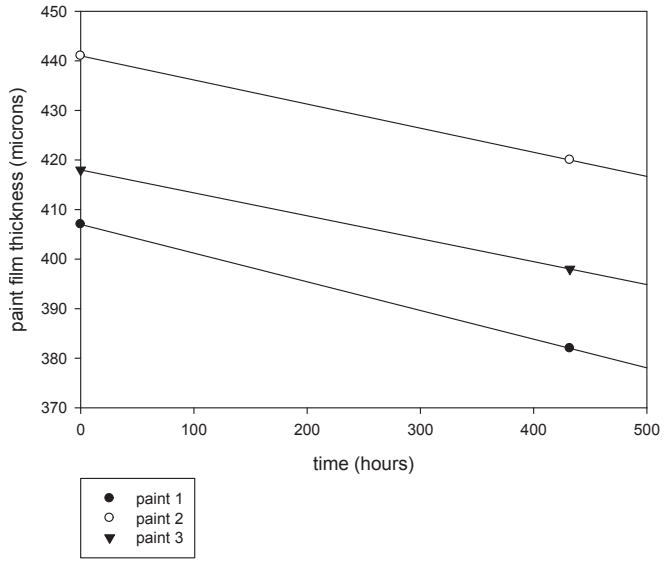

Fig. 12a. Antifouling Paint film depletion with time at drum speed of 450 rpm.

paint suitable painting schemes could be designed at regions of excessively high shear stresses and other niche areas to minimize the risk of antifouling paint failure and thereby increasing the risk of transmigration of invasive species.

A regression analysis for the three paints yielded a correlation of the form

$$y = ax + bx^2 + cx^3 + d \quad (1)$$

Where y = paint film depletion/hour.
Where x = wall shear stress (Pa)

The values of a b c and d are given in Table 2 for the paints tested.

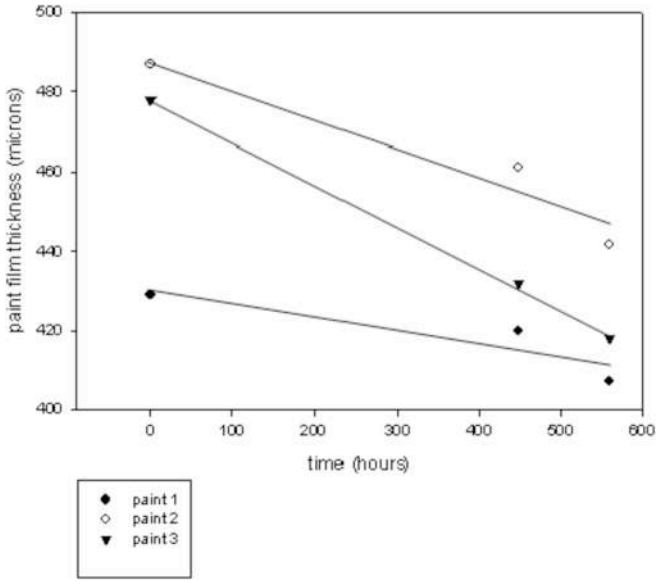

Fig. 12b. Antifouling Paint film depletion with time at drum speed of 550 rpm.

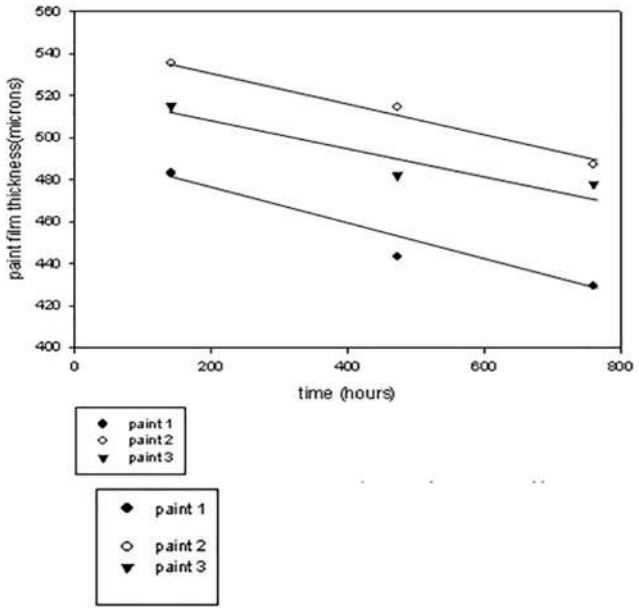

Fig. 12c. Antifouling Paint film depletion with time at drum speed of 690 rpm.

To obtain paint film depletion data with shear stresses for the vessel depicted in Fig. 3 it would take between three to five years using the present drum test apparatus. Therefore as mentioned earlier the drum test was run at speeds that correspond to much higher shear stresses and the results were extrapolated to very low values in the range of 10–50 Pa so as to obtain the corresponding paint film depletions computed for the vessel using equation. (1). This can be strictly justified since no experiments simulating exact operating conditions is possible. It must however be mentioned that certain conclusions derived from the drum test data as stated below are valid for full scale also:

(i) The depletion rate is linear with time
(ii) Though the Reynold's number is lower than that of ship it is in the turbulent region.
(iii) Shear stress can be related to paint film depletion in a non-linear manner.

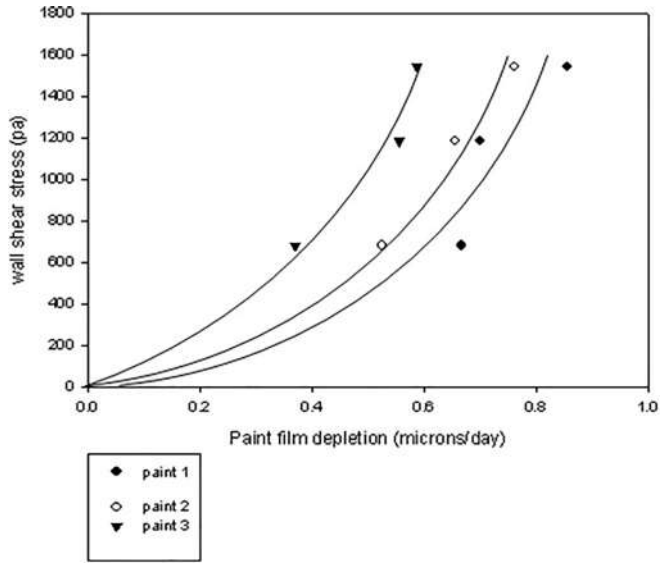

Fig. 13. Variation of paint film depletion with calculated wall shear stress.

Table 2
Parameters for equation (1).

Paint	a	b	c	d
1	3×10^{-4}	-2.69×10^{-7}	9.418×10^{-11}	-2.463×10^{-19}
2	2×10^{-4}	-1.236×10^{-7}	3.751×10^{-11}	1.656×10^{-19}
3	7.5×10^{-5}	-2.658×10^{-8}	-7.960×10^{-11}	6.089×10^{-19}

Table 3
Indicative antifouling coat thickness for various types of vessels.

Type of vessel	Dry-dock cycle (years)	Paint thickness (microns)
General cargo	five	250–300
Naval	Three	125–200
Coast guard	One	50–80

As mentioned earlier the current practice of antifouling paints is to paint the underwater hull surface with a uniform coat of predetermined thickness. The thickness of this coating is usually determined from experience by trial and error and approximate coating thicknesses for various vessels are indicated in Table 3. This practice has a number of drawbacks which include premature depletion of AF coating in niche areas where the wall shear stress is exceedingly high wastage of AF paint introducing toxic entities in the aquatic environment much above than that what is required for AF protection and cost of the additional quantity of paint that does not contribute to antifouling protection.

A correlation of the form of equation (1) which relates paint film depletion with wall shear stress would optimize the antifouling coat thickness at all locations on the vessels hull based on the wall shear stress at the corresponding locations. A possible antifouling paint scheme based on wall shear stresses and computed from equation (1) for the three AF paints is listed in Table 4.

8. Conclusion

A theoretical procedure has been suggested for determining wall shear stress on the underwater hull surface. An actual photographic record of a tanker in dry dock after 5 years of sailing has been compared with the theoretical results. The comparison indicates that the regions of high shear stress suffer from fast paint depletion which have not lasted for the 5 year period.

The results of the analysis show that paint 1 has the maximum polishing rates while in paint 3 the polishing action is minimum. This implies that paint 3 could be coated for high speed high activity vessels such as ocean going vessels while paint 1 would be an option for low speed low activity vessels such as harbour crafts motor launches etc.

Table 4
Wall shear stress and corresponding paint film thickness for Paints tested.

Wall Shear Stress (pa)	Thickness of paint film coating for 5-year dry-dock cycle (microns)		
	Paint 1	Paint 2	Paint 3
0–10	141	87	33
10–20	268	173	66
20–30	405	258	98
30–40	507	342	132

Although the above paint schemes were a result of extrapolation to very low values from experimental data they nevertheless establish a procedure for the computation of AF paint coating thickness throughout the underwater portion of the hull of the vessel. Such procedure could optimize the painting scheme that would not only reduce the costs of painting but would prevent excessive biocides from entering the aquatic/terrestrial environment due to superfluous and unutilized toxic paints.

To improve the accuracy of the results the drum-tests must be conducted at linear speeds that are close the actual speed of the vessel. Further various other hull forms must be investigated to identify zones of excessive wall shear stresses.

Funding

This work was supported by Department of Science & Technology Government of India (Sanction Order No: SR/S3/MERC-033/2010(g) dated 12th July 2011.

Acknowledgements

This paper is part of a project funded by the Department of Science and Technology Government of India and their contribution is gratefully acknowledged. The authors gratefully thank the staff of Indian Maritime University Visakhapatnam campus and suppliers of paint information from M/S Hindustan Shipyard Ltd. for the constant help and support during the course of the project. The authors also gratefully acknowledge the shipping company (name withheld) for providing the necessary photographs of paint depletion.

References

Almeida, E., Diamantino, T.C., Sousa, O., 2007. Marine Paints: the Particular Case of Antifouling Paints Progress in Organic Coatings, vol 59. pp. 2–20.
Anderson, C.D., 1993. Self-polishing antifoulings: a scientific perspective. In: Proceedings Ship Repair & Conversion. 93. pp. 1–17 London November 1993.
Ashton, G.V., Willis, K.J., Cook, E.J., Burrow, M., 2007. Distribution of the introduced amphipod Caprella mutica Shurin (Amphipoda: *Caprellida: Caprellidae*) on the west coast of Scotland and a review of its global distribution. Hydrobiologia 590, 31–41.
Brine, O., Hunt, L., Costello, M.J., 2013. Marine biofouling on recreational boats on swing moorings and berths. Manag. Biol. Invasions 4, 327–341.
Camps, M., Barani, A., Gregori, G., Bouchez, A., Le Berre, B., Bressy, C., Blache, Y., Briand, J., 2014. Antifouling coatings influence both abundance and community structure of colonizing biofilms: a case study in the northwestern Mediterranean sea. Appl. Environ. Biol. 80 (16), 4821–4831.
Chan, F.T., MacIsaac, H.J., Bailey, S.A., 2015. Can. J. Fish. Appl. Sci. 72 (8), 1230–1240.
Coutts, A.D.M., 1999. Hull Fouling as a Modern Vector for Marine Biological Invasions: Investigation of Merchant Vessels Visiting Northern Tasmania. MSc Thesis Australian Maritime College Tasmania.
Coutts, A.D.M., Piola, R.F., Hewitt, C.L., Connell, S.D., Gardner, J.P.A., 2010. Effect of vessel voyage speed on survival of biofouling organisms: implications for translocation of non indigenous marine species. Biofouling 26, 1–13.
Demirel, Y.K., Khorasanchi, M., Turan, O., Incecik, A., 2014. Prediction of the effect of hull fouling on ship resistance using CFD. In: 17th International Congress on Marine

Corrosion and Fouling, ICMCF 10-16 July 2014.
Drake, J.M., Lodge, D.M., 2007. Hull fouling is a risk factor for intercontinental species exchange in aquatic ecosystems. Aquat. Invasions 2 (2), 121–131.
Gollasch, S., 2002. The importance of ship hull fouling as a vector of species introductions into the North sea. Biofouling 18 (2), 105–121.
Hellio, C., Yebra, D., 2007. Advances in Marine Antifouling Coatings and Technologies. Woodhead Publishing Limited CambridgeUK.
Hewitt, C.L., 2002. The distribution and biodiversity of tropical Australian marine bioinvasions. Pac. Sci. 56 (2), 213–222.
Hunter, J.E., Cain, P., 1996. Antifouling coatings in the 1990s - environmental economic and legislative aspects. In: IMAS 96: Shipping and the Environment- Is Compromise Inevitable. Proc. IMarE Conf. Part 1. The Institute of Marine Engineers, London UK, pp. 61–78.
Jones, G., 2009. The Battle against Marine Biofouling : a Historical Review in Advances Inmarine Antifouling Coatings and Technology. Woodhead publishing limited ISBN 978-1-84569-386-2.
Kiil, S., Weinell, C.E., Pedersen, M.S., Dam-Johansen, K., 2001. Analysis of self-polishing antifouling paints using rotary experiments and mathematical modeling. Ind. Eng. Chem. Res. 40 (18) 3906 – 320.
Larsson, L., Raven, H.C., 2010. Ship Resistance and Flow Society of Naval Architects and Marine Engineers USA.
Ma, C., Zhang, W., Zhang, G., Qian, P., 2017. Environmentally friendly antifouling coatings Based on biodegradable polymer and natural antifoulant. ACS Sustain. Chem. Eng. 5 (7), 6304–6309.
Olivera, D., Granhag, L., 2016. Future work on drag and boundary layer properties of iofouling collected from commercial vessels. In: 1St Hull Performance & Insight Conference Castello di Pavone 13-15 April 2016.
Politis, G., Atlar, M., Williams, D., 2011. A state-of-the-art facility for the determination of polishing rate of SPC coatings. In: Proceedings of the 2nd International Conference on Advanced Model Measurement Technology for the Maritime Industry (AMT'11). Newcastle upon Tyne, UK.
Politis, G., Atlar, M., Kidd, B., Stenson, P., 2013. A multipurpose flume for the evaluation of hull coatings. In: Proceedings of the 3rd International Conference on Advanced Model Measurement Technology for the Maritime Industry (AMT'13). Gdansk, Poland.
Rainer, S.F., 1995. Potential for the Introduction and Translocation of Exotic Species by Hull Fouling: a Preliminary Assessment. Commonwealth Scientific and Research Organisation (CSIRO) Centre for Research on Introduced Marine Pests.Technical Report 1.HobartAustralia.
Yebra, D.M., Kiil, S., Dam_Johansen, K., Weinell, C., 2005. Reaction rate estimation of controlled-release paint binders: rosin based systems. Prog. Org. Coating 53, 256–275.